Tellus (1985), *37A*, 30–40

Simulation of the sea-breeze front with a model of moist convection

L. C. J. VAN DE BERG and J. OERLEMANS, *Institute of Meteorology and Oceanography, State University of Utrecht, Princetonplein 5, Utrecht 3508 TA, The Netherlands*

(Manuscript received December 20, 1983; in final form July 16, 1984)

ABSTRACT

Although in general the sea breeze can be considered as a mesoscale atmospheric circulation, the sea-breeze *front* has a much smaller scale. Simulation of the development of a sea-breeze front should therefore be preferably done with a non-hydrostatic model, with high spatial resolution (grid distances of a few hundred meters). Here we describe an attempt to do this. We conducted a few numerical experiments to study in an explicit way the effect of convective cloud formation on the evolution of the sea-breeze front. The model used is a 2-D cloud model, applied to a domain 60 km long and almost 4 km high, with a resolution of 250 m. Integrations were carried out over 4 h of simulated time.

We found that even with only a weak offshore background wind (1 m/s), the sea breeze rapidly takes on the form of a gravity current with a well-developed head. A comparison of runs with and without cloud simulation revealed that the formation of clouds tends to strengthen the sea breeze. The reason is that convective clouds form over land or just above the sea-breeze front, and dissipate at the seaward side of the front. The net effect is an additional horizontal gradient in diabatic heating.

1. Introduction

The sea-breeze circulation is a rather pure type of a thermally-driven circulation in the atmosphere, and it has been observed and studied for quite a long time. Early quantitative explanations of the sea breeze made use of simple linear models (Jeffreys, 1922; Schmidt, 1947; Haurwitz, 1947; among many others). In particular Walsh (1974) showed that a linear model of sufficient spatial resolution is able to recover the essential features of a sea-breeze circulation, even for different background situations.

Non-linear models have also been used widely, e.g. Estoque (1961), Fisher (1961), McPherson (1968), Neumann and Mahrer (1971), Pielke (1974). Studies carried out in more recent years have employed more general mesoscale numerical models to study the sea/land breeze circulation system for given orography and coastal geometry (e.g. Segal et al., Mahrer and Piekle, 1976). Se also Anthes (1983), for a review.

In all these studies, the sea breeze is considered as being essentially a circulation cell in a vertical plane, steadily increasing in size. Such a cell can be simulated reasonably well with a spatial resolution (on a grid) of the order of a few kilometers. However, it has been observed for a long time that in many cases the sea breeze sets in suddenly, in particular when the synoptic-scale wind is weakly offshore. In view of this, it seems more natural to consider the sea breeze as a gravity current with a well-defined head.This interpretation was particularly put forward by Simpson (1969).

Of course it takes some time before a sea-breeze front forms, because it owes its existence to the non-linear (advection) terms in the dynamic equations. A well-developed sea-breeze circulation is thus in fact characterized by *two* horizontal length scales, namely, the scale of the circulation cell and the scale of the front. This has some inplications for the type of models to be used for numerical simulation.

When primary interest is in the general sea-

breeze circulation, *hydrostatic* models should be sufficiently accurate. On the other hand, simualtion of a sea-breeze front requires a length scale of a few hundreds of meters to be resolved. The fact that a well-developed front has a horizontal (cross-front) scale of a few hundred meters makes it hard to believe that the dynamics of the frontogenesis process are hydrostatic. It has sometimes been argued that vertical accelerations are unimportant in sea-breeze circulations, but such conclusions were, to our knowledge, always based on grids with a few km spacing. The proper interpretation of such results seems to be that the model's grid parameter rather than the actual physical processes of the sea breeze permits one to employ the hydrostatic approximation.

Accepting the requirement of a horizontal resolution of a few hundreds of meters for a proper simulation of the sea-breeze front, the hydrostatic assumption has to be dropped. The simplest equations that can be used then is the anelastic set. However, dealing with vertical acceleration on a scale of 100 m also implies an explicit calculation of free convection as it normally occurs over land in sea-breeze situations. One can in fact expect considerable interaction between convective cells (and clouds) and a progressing sea-breeze front. It is well-know that strong convective cloud activity tends to develop over sea-breeze fronts (e.g. Pielke, 1974), but whether significant feedback on the frontal development occurs is an open question.

Fig. 1 shows an example of a well-defined sea-breeze front over the Netherlands. In this case, the pressure distribution was rather flat, leading to a very weak southerly wind over the coastal regions. Although the maximum land–sea surface temperature difference on this particular day was only about 4 K, a sharp front developed with strong associated convective cloud activity. It is tempting to assume that in this case the convective clouds help to strengthen the front.

In view of these considerations, we made an attempt to simulate the sea-breeze front by a 'cloud model', i.e. a high-resolution numerical model of

Fig. 1. IR-image from TIROS-N (22 July, 1983; 14:36 GMT), showing enhanced cumulus convection along a sea-breeze front in the western part of the Netherlands. Reproduced with permission of the University of Dundee.

moist convection. The principal difference between this investigation and previous ones is that motion is calculated in an absolutely unstable atmosphere. Where current sea-breeze models, hydrostatic or not, keep the atmosphere stratification stable by convective adjustment schemes, here the upward convective heat flux is calculated explicitly. Convective turbulence is generated over land. When the cold air overlying the sea starts to move inland, a situation occurs where organized motion (a gravity current) encounters an essentially turbulent motion field. This point should be kept in mind when comparing our flow patterns to the smooth velocity fields obtained in earlier numerical studies of the sea breeze.

The purpose of this model experiment is to see how a sea-breeze front forms, and how this depends on whether cloud formation occurs or not. It is not intended to simulate a full diurnal 'sea-breeze cycle'. This would not be possible, because the high resolution of the grid (250 m) allows only a limited domain to keep CPU-time reasonable. We carried out integrations over 4 h of simulated time, which appears to be long enough to study the formation and migration of the sea-breeze front.

2. Model description

The Boussinesq equation of motion serves as the basic equation for the model. It is combined with the incompressible continuity equation, a linearized equation of state, and a thermodynamic equation, to form the so-called 'shallow convection' set of equations. The derivation can be found in, among others, Dutton (1976; chapter 11), and will not be repeated here.

Since the flow is calculated in a vertical plane, perpendicular to the coastline a steamfunction ψ is used to describe the velocity field. The evolution of the flow is calculated from the vorticity equation (describing the vorticity component z perpendicular to the plane of the model flow).

Cloud physics are kept to a minimum. Cloud droplets form when the relative humidity exceeds 100%. The liquid water is advected by the wind; precipitation is not considered. Entrainment is parameterized by using a constant eddy diffusivity D for all quantities. This is computationally efficient, while simulated clouds still show all characteristic features of cumulus clouds (in particular, downdraughts generated by evaporative cooling are well simulated). In this study we used $D = 20\ \mathrm{m^2/s}$.

The vorticity equation is integrated by means of the Lax–Wendroff method (e.g. Mesinger and Arakawa, 1976).

When ζ has been obtained, a relaxation method is used to calculate the streamfunction from the Poisson equation $\nabla^2 \psi = \zeta$. From this, the velocity field is immediately derived. The velocity field is then used to do the thermodynamics in a Langrangian manner, i.e., from each grid point a backward trajectory is calculated along which the thermodynamic equation is applied (together with the moisture equations). For more detail the reader is referred to Van Delden and Oerlemans (1982).

The numerical experiments discussed here were carried out on a grid with 250 m spacing between grid points. A time step of 12 s was used. This makes the model expensive in use, but gives a very detailed simulation. The domain was 62.25 km long and 3.75 km high, giving a total number of grid points of 4016. The coastline was placed in the middle of the domain.

We now turn to the boundary conditions. At the surface, the air velocity is set to zero. Upward fluxes of heat and moisture are calculated according to a scheme suggested by Holtslag and Van Ulden (1983). We will not discuss this scheme, because the formulation of the surface layer is not critical to the present study; emphasis is on the internal dynamics.

At the top of the model atmosphere, situated above the inversion that dominates the initial stratification (see Section 3), temperature, mixing ratio, and the streamfunction are kept at constant values.

The lateral boundary conditions are more cumbersome. Because we want to carry out relatively long simulations, care has to be taken concerning reflection of gravity waves at the boundaries.

In order to obtain a scheme that allows gravity waves to propagate throught the boundaries, we included radiation-type boundary conditions, i.e.,

$$\frac{\partial \psi}{\partial t} + c \frac{\partial \psi}{\partial x} = 0. \tag{1}$$

The determination of the advection velocity c is the

difficult aspect. Various approaches have been proposed, with c either depending on model properties (grid distance, domain size, etc.) or on the simulated flow itself. (see, among others, Pearson, 1973; Klemp and Wilhelmson, 1978; Miller and Thorpe, 1981). We carried out tests with several formulations of c on a limited domain, and found that the method proposed by Miller and Thorpe (1981) performed best. It was included as follows.

A finite different replacement of eq. (1) is

$$\psi_b^{n+1} = \psi_b^n - c\frac{\Delta t}{\Delta x}(\psi_b^n - \psi_{b-1}^n), \tag{2}$$

where n is the time-step index, b the boundary grid point, Δt the time step and Δx the grid-point spacing. The advection velocity c is evaluated by rewriting eq. (2) for the previous time step, one grid point away from the boundary, i.e.

$$\psi_{b-1}^n = \psi_{b-1}^{n-1} - c\frac{\Delta t}{\Delta x}(\psi_{b-1}^{n-1} - \psi_{b-2}^{n-1}). \tag{3}$$

Eq. (3) is solved for c, and the value thus found is used in eq. (2) to calculate the new values of the streamfunction on the boundary.

This approach has one restriction, namely, the calculated advection velocity must be positive but smaller than $\Delta x/\Delta t$. For $c < 0$, inflow occurs, and the streamfunction on the boundary has to be prescribed. When horizontal derivatives are small, the advection velocity calculated from eq. (3) can be very large. In that case the stream function is taken constant in time.

In any numerical model, the scheme used is always a compromise between artificial damping and stability properties. The mixed Eulerian–Lagrangian approach we used enables infinitely long integrations to be carried out—if boundaries were not present. However, as in all cloud models, reflection of gravity waves at the boundaries ultimately effects the 'inner solution', unless extremely strong damping is used.

To give an impression of how the present model transmits gravity waves, Figs. 2 shows the result of a run on a small domain (20 km long), in which a train of gravity waves was forced in the middle of the domain. This was carried out by diabatic heating at a block of 8 × 4 grid points in the middle of the domain. The heating rate was 0.0017 K s^{-1}, applied for 5 min. To prevent convective instabilities from developing, an absolutely stable initial stratification was used (γ = 5 K/km). Because different behaviour can be expected at inflow and outflow boundaries, a background wind of 1 m/s was prescribed.

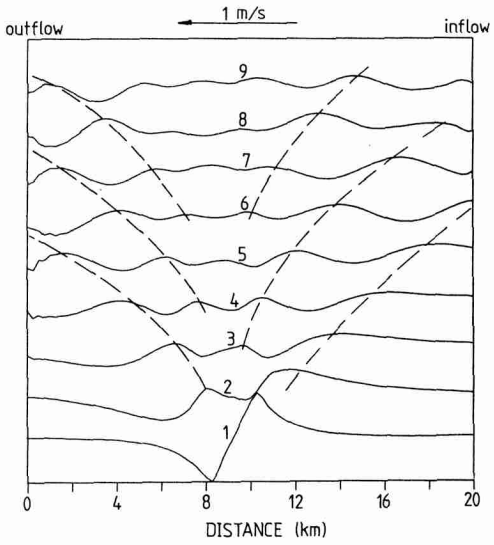

Fig. 2. A test run on a small domain in which gravity waves are generated by switching on a local heat source for a short time. Solid lines show the stream function at a height of 1000 m. Time interval between curves is 5 min. Vertical velocities associated with these gravity waves are typically 10 cm s^{-1}.

Fig. 2 displays the streamfunction ψ at a height of 1000 m. Different curves correspond to different times, the interval being 5 min. The evolution of ψ shows that the gravity waves run smoothly through the model domain. A typical vertical velocity is 10 cm s^{-1}. The damping appears to be reasonably small. Note the general increase of the wavelength (a non-linear effect) and the corresponding increase in phase velocity.

There are no problems at the inflow boundary, while at the outflow boundary some ripples occur after about 20 min of simulated time. The transmission of the waves through the boundaries of the domain appears to be satisfactory. From the figure it is also obvious that no noise is generated on small scales. Altogether, this test shows that the numerical scheme is stable, has only weak damping and absorbs gravity waves reasonably well at the boundaries.

Nevertheless, in the real sea-breeze simulations,

Table 1. *Grid resolution and size of some models used to simulate moist convection; the last column gives simulated time*

Reference	Δl (m)	Δz (m)	L (km)	H (km)	Time (min)
Schlesinger (1980	1700	700	49	14	48
Wilhelmson and Klemp (1978)	1500	500	36	10	90
Thorpe and Miller (1978)	1000	100 mb	29	900 mb	82
Tripoli and Cotton (1978)	750	750	35	17	60
This study	250	250	62	4	240

with a domain 62 km long, reflection of gravity waves disturbs the 'inner solution' after about 4 h. To show that this is not too bad, we list in Table 1 some other model experiments involving meso-scale-convective structures. Although most of these models are three-dimensional, the basic problem of reflection of gravity waves is not different in two-dimensional models. A typical ratio of horizontal domain size to integration time is 1 to $\frac{1}{4}$ km/min, corresponding to a velocity scale of 16.7 to 4.2 m/s. This is a typical fast gravity wave speed.

After this somewhat lengthy discussion of boundary conditions, we now turn to the numerical experiment. Although 4 h of simulated time is not a very long period, a sea-breeze front can easily form and migrate inland in such a time span.

3. The numerical experiment

As outlined in Section 1, the purpose of this study is to see in detail how the sea-breeze front forms, and what rôle convective clouds play. We conducted two experiments, with the same initial and boundary conditions, one with and one without cloud simulation. In this way, the effect of heating by condensation and evaporative cooling should show up. Since the purpose was not to carry out a real case study, a schematic initial state was used.

The initial temperature distribution over sea and land was prescribed as being identical, with an atmospheric lapse rate of 7.25 K km^{-1} up to a height of 2750 m, and a very strong inversion above this level (temperature increasing by 8 k up to the top of model domain). Such a situation is typical, although a bit exaggerated, for a mid-summer fine weather situation over western Europe (strong subsidence in a high-pressure cell), in which convective clouds are strongly restricted in their vertical development.

Surface fluxes of sensible heat and latent heat were simply estimated with a method described in Holtslag and Van Ulden (1983). For typical conditions we had in mind, the sensible heat flux over land was about 30 W m,$^{-2}$, and the latent heat flux about 70 W m^{-2}.

Over land, the sub-grid upward heat flux soon makes the stratification absolutely unstable. To enable convective motions to develop, random temperature perturbations, between −0.01 and 0.01 K, were imposed at all grid points.

In situations where well-developed sea-breeze fronts occur, the large-scale wind is generally offshore and weak. For that reason we imposed a 1 m s^{-1} offshore wind to the model.

Fig. 3 shows the evolution of the stream pattern for the run with cloud simulation (clouds are not displayed, close-ups will be given later). Dashed lines refer to positive values of the stream function. The first part of the integration is apparently dominated by the development of convective cells over land. At $t = 2$ h, a particular strong updraught is already seen in the vicinity of the coastline, and inland progression of a developing sea-breeze front begins. At $t = 3$ h the front has travelled over a distance of about 4 km. A typical wind speed behind the front is 4 m/s.

Although the offshore background wind is weak, the simulated sea-breeze circulation rapidly takes on the form of a typical gravity current. At its head, smaller-scale gravity waves are generated. They have a typical wavelength of about 6 km. Such gravity waves have been observed in many laboratory experiments, in which gravity currents are generated. An example is shown in Fig. 4. In this situation the waves break due to Kelvin–Helmholz instability. This is not observed in our model

Table 1. *Grid resolution and size of some models used to simulate moist convection; the last column gives simulated time*

Reference	Δl (m)	Δz (m)	L (km)	H (km)	Time (min)
Schlesinger (1980	1700	700	49	14	48
Wilhelmson and Klemp (1978)	1500	500	36	10	90
Thorpe and Miller (1978)	1000	100 mb	29	900 mb	82
Tripoli and Cotton (1978)	750	750	35	17	60
This study	250	250	62	4	240

with a domain 62 km long, reflection of gravity waves disturbs the 'inner solution' after about 4 h. To show that this is not too bad, we list in Table 1 some other model experiments involving meso-scale-convective structures. Although most of these models are three-dimensional, the basic problem of reflection of gravity waves is not different in two-dimensional models. A typical ratio of horizontal domain size to integration time is 1 to $\frac{1}{4}$ km/min, corresponding to a velocity scale of 16.7 to 4.2 m/s. This is a typical fast gravity wave speed.

After this somewhat lengthy discussion of boundary conditions, we now turn to the numerical experiment. Although 4 h of simulated time is not a very long period, a sea-breeze front can easily form and migrate inland in such a time span.

3. The numerical experiment

As outlined in Section 1, the purpose of this study is to see in detail how the sea-breeze front forms, and what rôle convective clouds play. We conducted two experiments, with the same initial and boundary conditions, one with and one without cloud simulation. In this way, the effect of heating by condensation and evaporative cooling should show up. Since the purpose was not to carry out a real case study, a schematic initial state was used.

The initial temperature distribution over sea and land was prescribed as being identical, with an atmospheric lapse rate of 7.25 K km^{-1} up to a height of 2750 m, and a very strong inversion above this level (temperature increasing by 8 k up to the top of model domain). Such a situation is typical, although a bit exaggerated, for a mid-summer fine weather situation over western Europe (strong subsidence in a high-pressure cell), in which convective clouds are strongly restricted in their vertical development.

Surface fluxes of sensible heat and latent heat were simply estimated with a method described in Holtslag and Van Ulden (1983). For typical conditions we had in mind, the sensible heat flux over land was about 30 W m,$^{-2}$, and the latent heat flux about 70 W m^{-2}.

Over land, the sub-grid upward heat flux soon makes the stratification absolutely unstable. To enable convective motions to develop, random temperature perturbations, between -0.01 and 0.01 K, were imposed at all grid points.

In situations where well-developed sea-breeze fronts occur, the large-scale wind is generally offshore and weak. For that reason we imposed a 1 m s^{-1} offshore wind to the model.

Fig. 3 shows the evolution of the stream pattern for the run with cloud simulation (clouds are not displayed, close-ups will be given later). Dashed lines refer to positive values of the stream function. The first part of the integration is apparently dominated by the development of convective cells over land. At $t = 2$ h, a particular strong updraught is already seen in the vicinity of the coastline, and inland progression of a developing sea-breeze front begins. At $t = 3$ h the front has travelled over a distance of about 4 km. A typical wind speed behind the front is 4 m/s.

Although the offshore background wind is weak, the simulated sea-breeze circulation rapidly takes on the form of a typical gravity current. At its head, smaller-scale gravity waves are generated. They have a typical wavelength of about 6 km. Such gravity waves have been observed in many laboratory experiments, in which gravity currents are generated. An example is shown in Fig. 4. In this situation the waves break due to Kelvin–Helmholz instability. This is not observed in our model

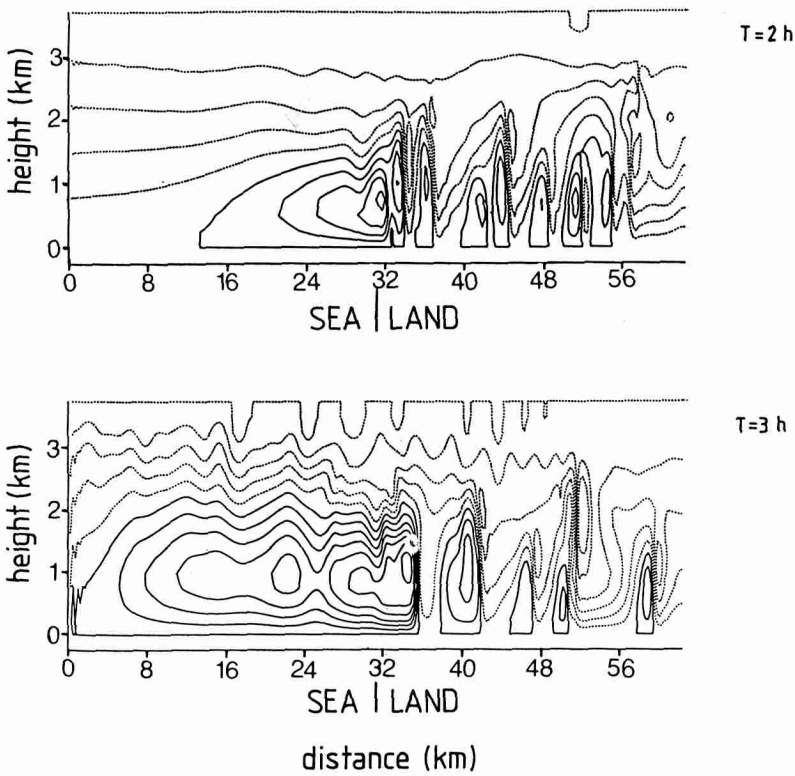

Fig. 3. Stream function for the run with cloud simulation, after 2 and 3 h of simulated time. Extremes encircled by solid lines correspond to counter-clockwise motion. Over land, the flow is dominated by convective cells (updraught velocities are up to 10 m s^{-1}), while over sea, the sea-breeze cell develops. Note the waves on top of the sea breeze (compare Fig. 4).

experiments, probably because the vertical shear at the top of the gravity current is not strong enough to overcome the diffusion.

At $t = 4$ h, reflection of gravity waves at the outflow boundary starts to effect the inner solution. The integration was therefore stopped at this point.

The interaction between the head of the gravity current and the convective cells is better seen in the series of close-ups shown in Fig. 5. The pictures give horizontal air velocity in the coastal region and are spaced at 5 min intervals. Clouds are also indicated. Note again that the flow is assumed to be incompressible, so the upward velocity gradient is directly proportional to the convergence of the horizontal wind.

At $t = 2^{50}$ h, a cumulus cloud with a depth of about 1200 m is found over the sea-breeze front. This cloud drifts in an offshore direction and evaporates rapidly, but another cloud is formed right over the head of the gravity current ($t = 3^{05}$ h). This cloud is in fact directly forced by the updraught at the sea-breeze front. During this period, the front is almost stationary. However, when the latter cloud also evaporates (it has disappeared at $t = 3^{10}$ h), the sea-breeze front migrates inland again. The last few pictures in the series show that this more rapid advance proceeds by the catching of a weak convective cell by the gravity current.

A few additional comments can be made on the basis of these flow patterns. Firstly, the head of the gravity current appears to vary in shape and significance depending on whether offshore drifting convective cells are encountered. Gravity wavelike structures appear at the interface of cold and warm air but their behaviour is irregular. Secondly, there seems to be no systematic increase in the depth of the gravity current. Due to the imposed strong

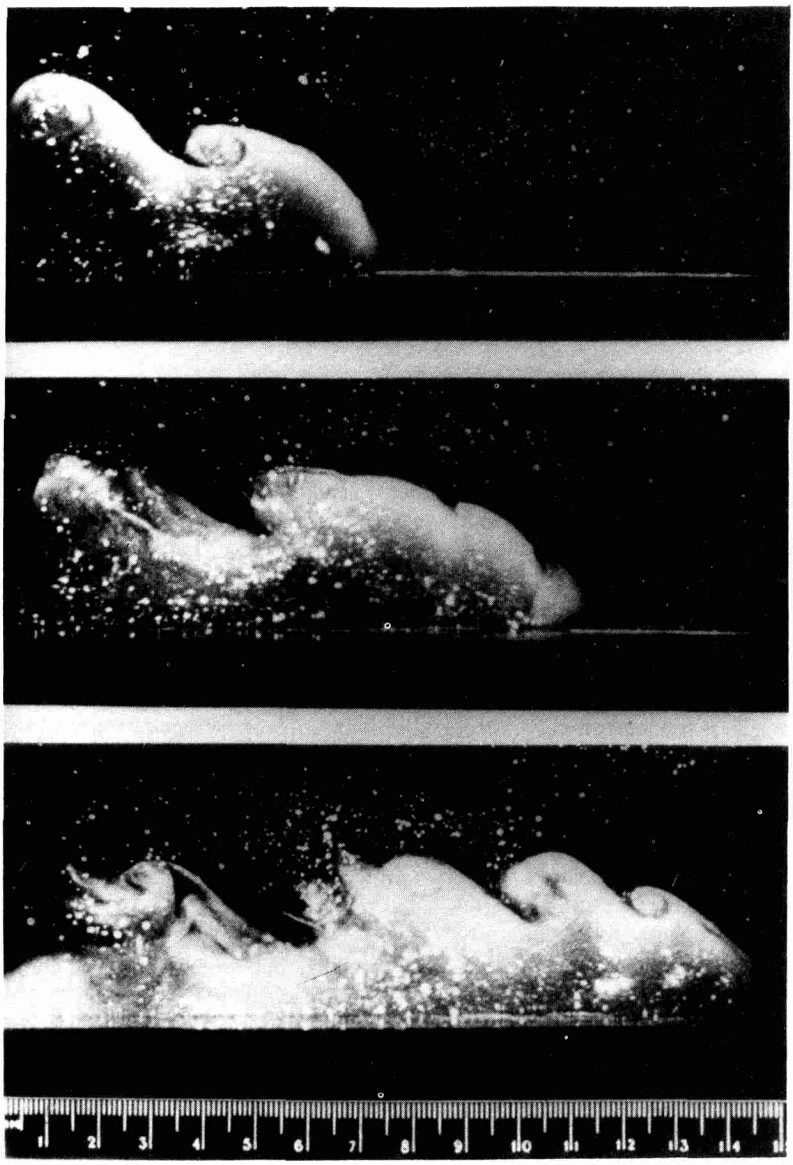

Fig. 4. Photographs of density current in a laboratory experiment (from Simpson, 1969). The presence of breaking waves at the interface is striking. Reproduced with permission of the Royal Meteorological Society.

temperature inversion in the initial state, a balance between onshore wind at lower levels and offshore wind over about the same depth below the inversion is rapidly established.

An overview of cloud development is shown in Fig. 6. Cloud cover (i.e. liquid water present at some height) is plotted as a function of x and simulated time. After about 1 h, small cumulus clouds appear; later, larger clouds dominate. The general advection of clouds from the right to the left is clearly seen. When clouds approach the frontal zone, they are accelerated in an offshore direction and subsequently evaporate. This acceleration is precisely what is observed so frequently in reality.

We finally consider the differences between the experiment discussed above and a run without

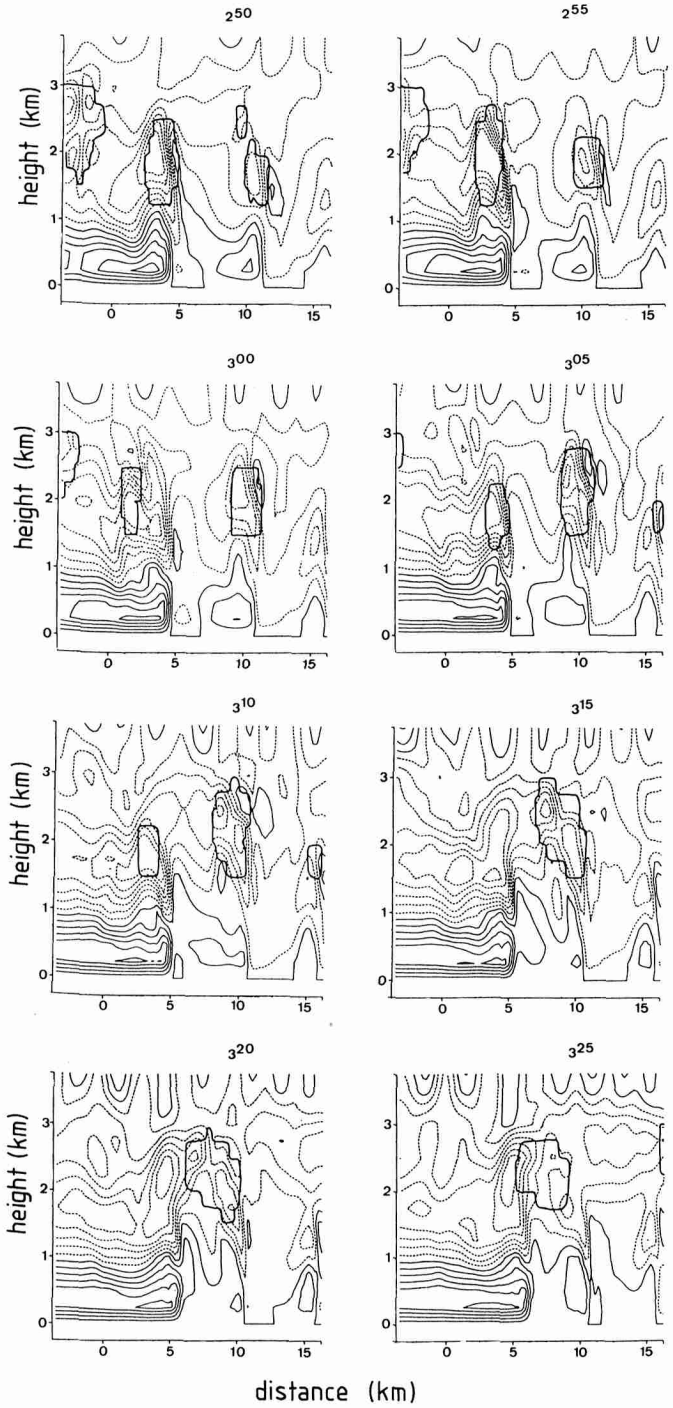

Fig. 5. Close ups of flow field and cloud formation in the vicinity of the sea-breeze front. Contours give horizontal wind (contour interval: 1 m s^{-1}); solid lines refer to flow from left to right, dashed lines from right to left. The coastline is at $x = 0$. Clouds are indicated by heavy lines.

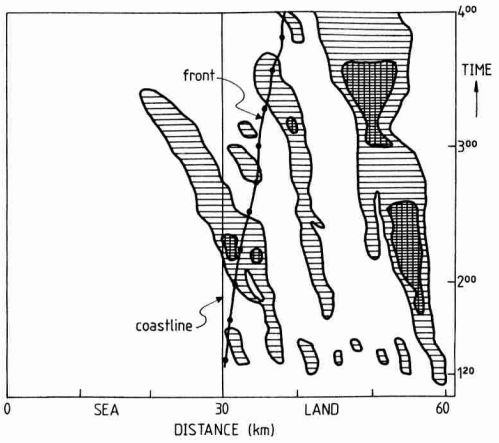

Fig. 6. Simulated cloud cover in a running-time diagram. The sea-breeze front is indicated by the line with dots.

cloud simulation, all other things being equal. Stream patterns for the no-cloud run will not be presented here, because the general picture is similar to the one already discussed. We found that in the no-cloud case, the sea-breeze was generally weaker. Although in the run with clouds, precipitation did not occur, the formation and evaporation of cumulus clouds appear to have a non-negligible effect on the development of the sea breeze. The area of the circulation cell in the no-cloud case was typically $\frac{3}{4}$ of the area in the case with cloud simulation.

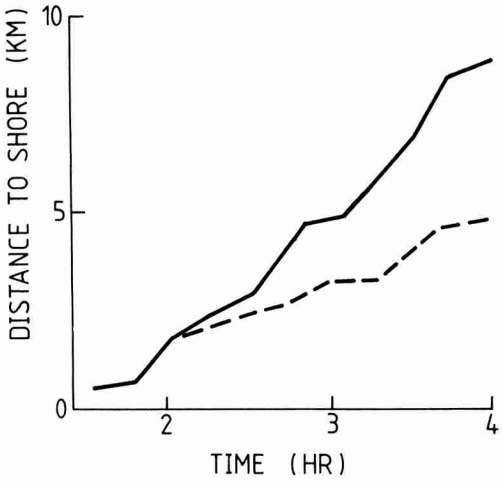

Fig. 7. Inland migration of the sea-breeze front, in the case with cloud simulation (solid line) and without cloud simulation (dashed line).

The difference between the experiments also showed up clearly in the progression of the sea-breeze front. In Fig. 7, the distance of the front to the shoreline is plotted as a function of time. Although determining the position of the front involves some ambiguity, the difference between cloud and no-cloud cases is certainly significant. Obviously, the inland migration of the sea breeze proceeds at a higher rate when cloud forma-tion is included.

4. Conclusions and discussion

In our view, this study demonstrates the feasibility of a model of moist convection to study the evolution of the sea-breeze front. In spite of its two-dimensionality, the behaviour of simulated convective clouds in relation to the development of the sea-breeze cell looks very realistic. The sea-breeze front apparently has a typical length scale comparable to that of the convective elements, and its migration is therefore not smooth in time. So the use of a model in which convection is calculated explicitly adds a new aspect to the simulation of sea-breezes.

As a major conclusion, we mention the fact that the simulated sea-breeze rapidly takes the form of a pure gravity current, with a well-defined head, in accordance with laboratory experiments (e.g. Simpson, 1969). Although the offshore background wind is weak, the solenoidal circulation around the coastline very soon exhibits a strong asymmetry. This asymmetry cannot be solely explained on the basis of linear distortion of the circulation by the background wind. Apparently, the non-linear advection terms very soon dominate.

A second conclusion involves the rôle of cloud formation in migration of the sea-breeze front. The front moves inland in an essentially turbulent model atmosphere, and it is difficult to pin down precisely why the front moves more rapidly when cloud formation is included. A global interpretation can be given, however. Clouds form on the landward side of the front, and generally evaporate at the seaward side. This implies the existence of an additional horizontal gradient in diabatic heating. Latent heat is relaased in the convective air over land and just above the front, while evaporative

cooling occurs at the seaward side. This obviously will enforce the sea-breeze circulation.

To make this more concrete, we calculated the gradient in diabatic heating rate across the front, from the model output. The actual quantity considered is the difference between mean heating rate at the right-hand side of the front and at the left hand side of the front, scaled with the differential heating rate due to the surface-sensible heat flux over land. So this quantity directly gives the contribution to the forcing originating from the water phase transitions. It is plotted as a function of time in Fig. 8. Although the curve is very irregular, the net effect is not negligible: it amounts to about 30% of the 'direct' forcing by the sensible heat flux.

In view of the results presented here, a further comment on Fig. 1 is in order. In this example, the area where the cumulus clouds develop has a very sharp boundary at the seaward side, in contrast to the result shown in Fig. 6. We believe that this has to do with the initial stratification. During various field experiments in sea-breeze situations (results unpublished) we have observed accelerating clouds evaporating in a random manner over sea. This type of behaviour is only observed when a strong inversion, limiting the depth of the convective clouds, is present. When the stratification is less stable, and clouds may become deep and even precipitating, cloud patterns are more like the one shown in Fig. 1. The sea-breeze circulation becomes deeper, and the dynamics of the front will be different. In the Netherlands, and probably in general at midlatitudes, the shallow sea breeze occurs much more frequently, because sea-breeze situations are associated with the passage of anticyclones in which strong subsidence is present.

In the present model, the effect of the Coriolis force, interception of solar radiation by clouds, variations of the surface fluxes with soil properties, orography, etc. were not included. Such factors may of course affect the development and migration of the sea-breeze front in a substantial way.

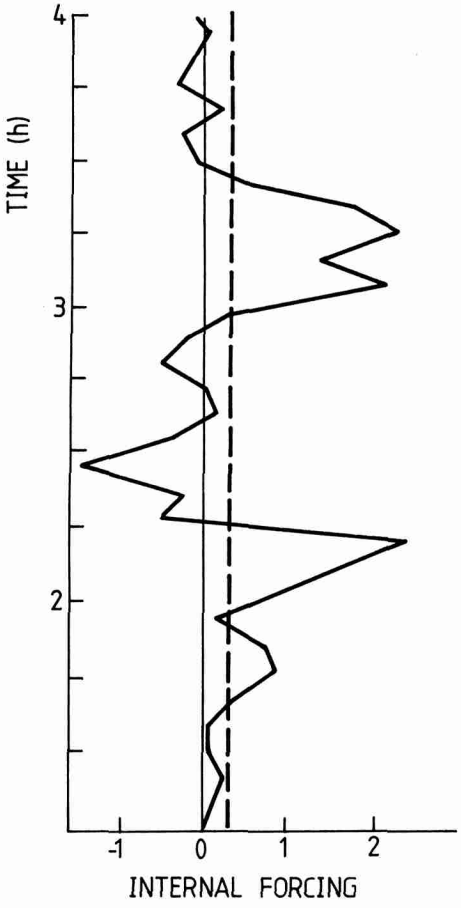

Fig. 8. Forcing due to cloud formation and evaporation, scaled with the forcing due to the sea-land difference in sensible heat flux at the surface. The internal forcing is highly variable; its mean value is given by the dashed line.

Further work will concentrate on such refinements, and will hopefully give some insight into why inland penetration of the sea breeze varies so strongly from place to place.

REFERENCES

Anthes, R. A. 1983. Regional models of the atmosphere in middle latitudes. *Mon. Wea. Rev. 111*, 1306–1335.

Dutton, J. A. 1976. *The ceaseless wind.* McGraw-Hill (New York), 579 pp.

Estoque, M. A. 1961. A theoretical investigation of the sea breeze. *Q. J. R. Meteorol. Soc. 87*, 136–146.

Fisher, E. L. 1961. A theoretical study of the sea breeze. *J. Meteorol. 18*, 216–233.

Haurwitz, B. 1947. Comments on the sea-breeze circulation. *J. Meteorol. 4*, 1–8.

Holtslag, A. A. M. and Van Ulden, A. P. 1983. A simple scheme for daytime estimates of the surface fluxes from routine weather data. *J. Clim. Appl. Meteorol. 22*, 517–529.

Jeffreys, H. 1922. On the dynamics of wind. *Q. J. R. Meteorol. Soc. 48*, 29–46.

Klemp, J. and Wilhelmson, R. 1978. The simulation of three-dimensional convective storm dynamics. *J. Atmos Sci. 35*, 1070–1096.

Mahrer, Y. and Pielke, R. A. 1976. Numerical simulation of the airflow over Barbados. *Mon. Wea. Rev. 104*, 1392–1402.

McPherson, R. D. 1968. *A three-dimensional numerical study of the Texas coast sea breeze.* Report 15, College of Engineering, University of Texas, 254 pp.

Mesinger, F. and Arakawa, a. 1976. *Numerical methods used in atmospheric models.* WMO GARP Publ. No. 17, Geneva.

Miller, M. J. and Thorpe, A. J. 1981. Radiation conditions for the lateral boundaries of limited area numerical models. *Q. J. R. Meteorol. Soc. 107*, 615–628.

Neumann, R. J. and Mahrer, B. A. 1971. A theoretical study of the land and sea-breeze circulation. *J. Atmos. Sci. 28*, 532–542.

Pearson, R. A. 1973. Properties of the sea-breeze front as shown by a numerical model. *J. Atmos. Sci. 30*, 1050–1060.

Pielke, R. A. 1974. A three-dimensional numerical model of the sea breezes over south Florida. *Mon. Wea. Rev. 102*, 115–139.

Schlesinger, R. E. 1980.A three-dimensional numerical model of an isolated thunderstorm. Part II: dynamics of updraft splitting and mesovortex evolution. *J. Atmos. Sci. 37*, 395–420.

Schmidt, F. H. 1947. An elementary theory of the land and sez breeze circulation. *J. Meteorool. 4*, 9–15.

Segal, M., Mahrer, Y. and Pielke, R. A. 1981. A three-dimensional numerical model study of summer meteorological patterns over the southeastern coasts of the Mediterranean Sea. Proc. of First International Conference on Meteorology and Air/Sea interaction of the Coastal Zone, The Hague, AMS, 404 pp.

Simpson, J. E. 1969. A comparison between laboratory and atmospheric density currents. *Q. J. R. Meteorol. Soc. 95*, 758–765.

Thorpe, A. J. and Miller, M. J. 1978. Numerical simulations showing the rôle of the downdraught in cumulonimbus motion and splitting. *Q. J. R. Meteorol. Soc. 104*, 873–893.

Tripoli, G. and Cotton, W. R. 1978. Cumulus convection in shear flow: three-dimensional numerical experiments. *J. Atmos. Sci. 35*, 1503–1521.

Van Delden, A. and Oerlemans, J. 1982. Grouping of clouds in a numerical cumulus convection model. *Beitr. Phys. Atmos. 55*, 239–252.

Walsh, J. E. 1974. Sea breeze theory and applications. *J. Atmos. Sci. 31*, 2013–2036.

Wilhelmson, R. B. and Klemp, J. B. 1978. A numerical study of storm splitting that leads to long-lived storms. *J. Atmos. Sci. 35*, 1974–1986.